QUT Digital Repository:
http://eprints.qut.edu.au/

QUT

This is the author version published as:

Novel ruthenium bipyridyl dyes with S-donor ligands and their application in dye-sensitized solar cells

Keri L. McCall[a], James R. Jennings[b], HongxiaWang[b], Ana Morandeira[c], Laurence M. Peter [b], James R. Durrant[c], Lesley J. Yellowlees[a], J. DerekWoollins [d], Neil Robertson[a*]

[a] School of Chemistry, University of Edinburgh, King's Buildings, Edinburgh, UK

[b] Department of Chemistry, University of Bath, Bath BA2 7AY, UK

[c] Centre for Electronic Materials and Devices, Department of Chemistry, Imperial College London, London SW7 2AZ, UK

[d] School of Chemistry, University of St. Andrews, North Haugh, St. Andrews, Fife KY16 9ST, UK

A b s t r a c t

Two series of novel ruthenium bipyridyl dyes incorporating sulfur-donor bidentate ligands with general formula [Ru(R-bpy)2C2N2S2] and [Ru(R-bpy)2(S2COEt)][NO3] (where R =H, CO2Et, CO2H; C2N2S2 = cyanodithioimidocarbonate and S2COEt = ethyl xanthogenate) have been synthesized and characterized spectroscopically, electrochemically and computationally. The acid derivatives in both series (C2N2S2 3 and S2COEt 6) were used as a photosensitizer in a dye-sensitized solar cell (DSSC) and the incident photo-to-current conversion efficiency (IPCE), overall efficiency (_) and kinetics of the dye/TiO2 system were investigated. It was found that 6 gave a higher efficiency cell than 3 despite the latter dye's more favorable electronic properties, such as greater absorption range, higher molar extinction coefficient and large degree of delocalization of the HOMO. The transient absorption spectroscopy studies revealed that the recombination kinetics of 3 were unexpectedly fast, which was attributed to the terminal CN on the ligand binding to the TiO2, as evidenced by an absorption study of R =H and CO2Et dyes sensitized on TiO2, and hence leading to a lower efficiency DSSC.

1. Introduction

With the need for alternative energy sources a key focus in today's world the scientific community has been challenged with finding the solution to the energy crisis. Solar energy is one area which has received significant attention in recent years, however the current high cost of the conventional inorganic solar cells has led

to extensive research into low cost alternatives. Dye-sensitized solar cells (DSSCs) have shown great promise in this field since the early 1990s [1], as they have the potential for high efficiency, low cost and ease of manufacture. The main components of a DSSC are a nanocrystalline semiconductor, generally titanium dioxide, sensitized with a dye and a redox electrolyte, such as iodide/triiodide (I−/I3−), as well as a platinum counter electrode. Optimization of all components and increased understanding of all electron transfer processes that occur in the cell is required in order to maximize the overall efficiency, with a significant amount ofwork focused on the optimization of the sensitizer [2]. Ruthenium bipyridyl complexes are of particular interest as a photosensitizer in this application due to their favorable photoelectrochemical properties and high stability in the oxidized state. Current high efficiency DSSCs utilize the sensitizer N719 (cis-bis(isothiocyanato)bis(2,2_-bipyridyl-4,4_- dicarboxylato)-ruthenium(II)bis-tetrabutylammonium) and have achieved a record efficiency of over 10% [3]. The disadvantage of this dye is the lack of absorption in the red and near-infrared region of the electromagnetic spectrum. The absorption spectra of ruthenium polypyridyl systems can be tuned by careful consideration of the HOMO and LUMO energy levels [4–6]. One can tune these levels in a number of ways, either by incorporation of a ligand with low-lying π^* molecular orbital or via the use of strongly electron donating ligands to destabilize the Ru t2g orbitals, both causing a decrease in the HOMO–LUMO gap and hence a red-shift in the absorption spectrum. The disadvantage of the former method is that the LUMOcan be shifted to a level belowwhich charge injection into the TiO2 conduction band can occur [7,8]. Another disadvantage of N719 is the potential dissociation of the monodentate NCS ligand, which will reduce the life span of the cell [9]. In this study the focus is on the use of bidentate S-donor ligands to increase the long-term

stability of the dye in a DSSC and also red-shift the absorption range of the system. A similar approach has been employed previously, for example, a series of ruthenium complexes with dithiocarbamate ligands were investigated for their performance in a DSSC and found to have the desired increase in absorption range. However the regeneration of the oxidized dyes by the iodide/triiodide electrolyte was found to be slow, resulting in charge recombination competing efficiently with dye regeneration in portions of the film where the iodide concentration was depleted, and hence a lower photocurrent was observed for these cells [10]. Dithiolate ligands have also been studied in this context and again were found to have an increased absorption range but low efficiencies were obtained due to fast charge recombination and slow dye regeneration [11]. This study focuses on the use of two ligands; potassium cyanodithioimidocarbonate (K2C2N2S2) and potassium ethyl xanthate (KS2COEt), in an attempt to build on the previous work with similar S-donor ligands and to enhance the electronic properties of the dyes. Six complexes (Fig. 1) have been synthesized and characterized electrochemically, spectroscopically andcomputationally using the two S-donor ligands. The unsubstituted and ester bipyridyl derivatives were synthesized to aid the study and rationalization of the electronic properties of the dye series, in particular due to the poorer solubility of the acid dyes, the electronic properties of these can be conveniently inferred fromthe ester analogues. The acid derivatives were used as a sensitizer in a DSSC, with the performance and kinetics of these devices investigated.

2. Experimental
2.1. General

The synthesis of $Ru(bpy)_2Cl_2$, [i] $Ru(decbpy)_2Cl_2$, [ii] and potassium cyanodithioimidocarbonate [iii] were carried out according to literature procedures. $RuCl_3.3H_2O$ was obtained from Johnson Matthey and all other chemicals were

purchased from Aldrich and used as received. Electrochemistry was carried out using a Pt working electrode, Pt rod counter electrode and Ag/AgCl reference electrode. All electrochemical experiments were carried out in either DMF or DCM and the supporting electrolyte used was TBABF$_4$ (0.1 or 0.3 M respectively). After each experiment the reference electrode was calibrated against the ferrocene/ferrocenium couple which was found to be at 0.55 V. The absorption spectra were recorded using a Perkin-Elmer Lambda 9 spectrophotometer controlled using the UV/Winlab software. Emission spectra were recorded at room temperature with dilute solutions of the dyes in ethanol, using a Fluoromax 2 fluorometer controlled by the ISAMain software. Spectroelectrochemical measurements were recorded at -40 °C using a 0.5 mm Pt gauze working electrode, Pt wire counter electrode and a Ag/AgCl reference electrode. Density functional theory calculations of the ester analogues were performed using the Gaussian 03 program [iv] with the starting structure input using the builder program Arguslab. The Becke three parameters hybrid exchange and the Perdew-Wang 1991 correlation functionals (B3PW91) level of theory were used.[v,vi] For the ruthenium atom a Hay-Wadt VDZ (n+1) ECP was used[vii] and all other atoms were described by 6-31G*.[viii] A frequency calculation was performed to ensure the optimized structures were minima on the potential energy surface, verified by the absence of negative values. TD-DFT was performed in a DMF polarizable continuum model,[ix] with the first 70 singlet transitions calculated. To make the DSSCs titanium dioxide paste (Solaronix, Ti-Nanoxide T) was deposited onto cleaned fluorine doped tin oxide conductive glass (TEC 15, Pilkington, UK) by doctor-blading. The film was dried at 100 °C for 15 minutes and then sintered at 450 °C for 30 minutes to remove the organics and to form a mesoporous film structure. The thickness of the film was about 12 μm. The films were sensitized with **3** and **6** using a 0.5 mM solution of the

dye in methanol. The platinized counter electrode was fabricated following the previously reported procedure.[x] A sandwich-structured cell was assembled by sealing the dye coated TiO_2 electrode and Pt electrode together by a thermal plastics spacer (Surlyn 1702, 25 μm, Solaronix) at 120°C. The electrolyte was introduced into the cell through the two holes which were drilled in the counter electrode. The holes were subsequently sealed by the thermal plastics (Surlyn 1702, Solaronix) combined with a piece of microscope slide under heat press. The active area of the cell was 1 cm^2. Transient absorption decays were measured using the "flash photolysis" technique. The sample was excited with a dye laser (Photon Technology International Inc., GL-301) pumped by a nitrogen laser (Photon Technology International Inc., GL-3300). The excitation wavelength was 500 nm, the pulse width was 800 ps, the fluence was about 50 μJcm^{-2} and the repetition frequency was 1 Hz. A 100-W tungsten-halogen lamp (Bentham, IL1) with a stabilized power supply (Bentham, 605) was used as a probe light source. The probe light passing through the sample was detected with a silicon photodiode (Hamamatsu Photonics, S1722-01). The signal from the photodiode was pre-amplified and sent to the main amplification system with an electronic band-pass filter to improve signal to noise ratio (Costronics Electronics). The amplified signal was collected with a digital oscilloscope (Tektronix, TDS 220), which was synchronized with a trigger signal of the laser pulse from a photodiode (Thorlabs Inc., DET210). To reduce stray light, scattered light and emission from the sample, two monochromators and appropriate optical cut-off filters were placed before and after the sample. Owing to the amplification and noise reduction system, the detectable change of absorbance was as small as 10^{-5} to 10^{-6}.

2.1.1. Synthesis of [Ru(bpy)2(C2N2S2)] (1)

Ru(bpy)$_2$Cl$_2$ (100 mg, 0.2 mmol) was dissolved in methanol (10 ml) and silver nitrate (71 mg, 0.4 mmol) in water (1 ml) was added. The mixture was refluxed for 1

hour, under N_2 and in reduced light, yielding a scarlet red solution and a white precipitate. The precipitate was removed by centrifugation and to the filtrate was added $K_2C_2N_2S_2$ (31 mg, 0.2 mmol) in water (1 ml). The mixture was stirred overnight, under N_2 and reduced light. The red precipitate was collected, washed with methanol and dried in vacuo. Yield: 49 mg, 46 %. Anal. Calc. for $C_{22}H_{16}N_6S_2Ru.H_2O$: C, 48.25; H, 3.30; N, 15.35. Found: C, 48.08; H, 2.76; N, 15.11. +ve FAB-MS: m/z 530 (M^+). ^{1}H-NMR (DMSO, 360 MHz): δ 9.48 (d, J_{HH} = 5.69, 2H), 8.53 (d, J_{HH} = 7.68, 2H), 8.44 (d, J_{HH} = 7.91, 2H), 7.92 (t, J_{HH} = 7.79, 2H), 7.67 (q, J_{HH} = , 4H), 7.50 (d, J_{HH} = 5.715, 2H), 7.10 (t, J_{HH} = 6.56, 2H).

2.1.2. Synthesis of [Ru(decbpy)2(C2N2S2)] (2)

Ru(decbpy)$_2$Cl$_2$ (100 mg, 0.12 mmol) was dissolved in methanol (10 ml) and silver nitrate (44 mg, 0.24 mmol) in water (1 ml) was added. The mixture was refluxed for 1 hour, under N_2 and in reduced light, yielding a deep red solution and a white precipitate. The precipitate was removed by centrifugation and to the filtrate was added $K_2C_2N_2S_2$ (30 mg, 0.2 mmol) in water (1 ml). The mixture was stirred overnight, under N_2 and reduced light. The dark red precipitate was collected, washed with methanol and dried in vacuo. Yield: 73 mg, 74 %. The product was further purified via a Sephadex LH-20 column using a 1:1 methanol:acetonitrile solution as the eluent. Anal. Calc. for $C_{34}H_{32}N_6O_8S_2Ru.2MeOH$: C, 46.31; H, 3.66; N, 9.53. Found: C, 45.09; H, 3.82; N, 9.71. +ve FAB-MS: m/z 818.2 (M^+). ^{1}H-NMR (DMSO, 360 MHz): δ 10.00 (d, J_{HH} = 6, 2H), 9.29 (s, 2H), 9.19 (s, 2H), 8.47 (d, J_{HH} = 6, 2H), 8.10 (d, J_{HH} = 5.9, 2H), 7.80 (d, J_{HH} = 5.9, 2H), 4.68 (q, J_{HH} = 7.1, 4H), 4.52 (q, J_{HH} = 7.1, 4H), 1.60 (t, J_{HH} = 7.1, 6H), 1.48 (t, J_{HH} = 7.1, 6H).

2.1.3. Synthesis of [Ru(dcbpy)2(C2N2S2)] (3)

Ru(decbpy)$_2$Cl$_2$ (100 mg, 0.12 mmol) was dissolved in methanol (10 ml) and silver nitrate (44 mg, 0.24 mmol) in water (1 ml) was added. The mixture was refluxed for

1 hour, under N_2 and in reduced light, yielding a deep red solution and a white precipitate. The precipitate was removed by centrifugation and to the filtrate was added 0.1 M aq. KOH (3 ml). The mixture was stirred for 10 minutes followed by the addition of $K_2C_2N_2S_2$ (30 mg, 0.2 mmol) in water (1 ml). The mixture was stirred overnight, under N_2 and reduced light. The product was precipitated with 1 M HCl (1 ml) yielding a dark red precipitate. Yield: 73 mg, 80 %. The crude product was further purified via a Sephadex LH-20 column using water as the eluent. Anal. Calc. for $C_{26}H_{16}N_6O_8S_2Ru.5H_2O$: C, 39.25; H, 3.29; N, 10.56. Found: C, 39.42; H, 2.93; N, 9.50. –ve ESI-MS: m/z 705 (M^+) ^{1}H-NMR (DMSO, 360 MHz): δ 9.83 (d, J_{HH} = 5.9, 2H), 9.08 (s, 2H), 8.99 (s, 2H), 8.28 (d, J_{HH} = 5.9, 2H), 7.92 (d, J_{HH} = 5.9, 2H), 7.63 (d, J_{HH} = 5.9, 2H)

2.1.4. Synthesis of [Ru(bpy)2(S2COEt)][NO3] (4)

$Ru(bpy)_2Cl_2$ (100 mg, 0.2 mmol) was dissolved in methanol (10 ml) and silver nitrate (71 mg, 0.4 mmol) in water (1 ml) was added. The mixture was refluxed for 1 hour, under N_2 and in reduced light, yielding a scarlet red solution and a white precipitate. The precipitate was removed by centrifugation and to the filtrate KS_2COEt (30 mg, 0.2 mmol) in water (1 ml). The mixture was stirred overnight, under N_2 and reduced light. The reaction mixture was concentrated and loaded onto a Sephadex LH-20 column, using methanol as the eluent. The main scarlet red band was collected. Yield: 102 mg, 85 %. Anal. Calc. for $C_{24}H_{25}N_5O_5S_2Ru.1MeOH$: C, 45.85; H, 4.01; N, 11.1. Found: C, 45.97; H, 3.34; N, 7.08, +ve FAB-MS: m/z 535 (M^+-NO$_3$), ^{1}H-NMR (DMSO, 360 MHz): δ 9.43 (d, J_{HH} = 5.67, 2H), 8.92 (d, J_{HH} = 8.3, 2H), 8.83 (d, J_{HH} = 7.91, 2H), 8.35 (t, J_{HH} = 7.09, 2H), 8.11 (t, J_{HH} = 7.48, 2H), 8.02 (t, J_{HH} = 6.62, 2H), 7.84 (d, J_{HH} = 5.61, 2H), 7.51 (t, J_{HH} = 6.6, 2H), 4.74 (q, J_{HH} = 7, 2H), 1.52 (t, J_{HH} = 7.06, 3H).

2.1.5. Synthesis of [Ru(decbpy)2(S2COEt)][NO3] (5)

Ru(decbpy)$_2$Cl$_2$ (100 mg, 0.12 mmol) was dissolved in methanol (10 ml) and silver nitrate (44 mg, 0.24 mmol) in water (1 ml) was added. The mixture was refluxed for 1 hour, under N$_2$ and in reduced light, yielding a deep red solution and a white precipitate. The precipitate was removed by centrifugation and to the filtrate was KS$_2$COEt (19 mg, 0.12 mmol) in water (1 ml). The mixture was stirred overnight, under N$_2$ and reduced light. The reaction mixture was concentrated and loaded onto a Sephadex LH-20 column using methanol as the eluent, with the main red band collected. The product was further purified by recrystallisation in ethyl acetate. Yield: 24 mg, 23 % Anal. Calc. for C$_{35}$H$_{37}$N$_5$O$_{12}$S$_2$Ru: C, 47.51; H, 4.21; N, 7.91. Found: C, 46.42; H, 3.45; N, 4.27, +ve FAB-MS: m/z 823 (M$^+$-NO$_3$), ^{1}H-NMR (DMSO, 360 MHz): δ 9.49 (d, J_{HH} = 6, 2H), 9.24 (s, 2H), 9.13 (s, 2H), 8.56 (d, J_{HH} = 6, 2H), 7.98 (d, J_{HH} = 6, 2H), 7.69 (d, J_{HH} = 6, 2H), 4.52 (q, J_{HH} = 7, 2H), 4.37 (q, J_{HH} = 7, 2H), 1.38 (t, J_{HH} = 7, 3H).

2.1.6. Synthesis of [Ru(dcbpy)$_2$(S$_2$COEt)][NO$_3$] (6)

Ru(decbpy)$_2$Cl$_2$ (100 mg, 0.12 mmol) was dissolved in methanol (10 ml) and silver nitrate (44 mg, 0.24 mmol) in water (1 ml) was added. The mixture was refluxed for 1 hour, under N$_2$ and in reduced light, yielding a deep red solution and a white precipitate. The precipitate was removed by centrifugation and to the filtrate was added 0.1 M aq. KOH (3 ml). The mixture was stirred for 10 minutes followed by the addition of KS$_2$COEt (38 mg, 0.12 mmol) in water (1 ml). The mixture was stirred overnight, under N$_2$ and reduced light. The product was precipitated with 1 M HCl (2 ml) yielding a dark red precipitate. Yield: 57 mg, 61 %. The crude product was further purified via a Sephadex LH-20 column using water as the eluent. Anal. Calc. for C$_{27}$H$_{33}$N$_5$O$_{18}$S$_2$Ru.6H$_2$O: C, 36.82; H, 3.78; N, 7.95. Found: C, 35.19; H, 2.00; N, 8.18, +ve ESI-MS: m/z 711 (M$^+$-NO$_3$), ^{1}H-NMR (DMSO, 360 MHz): δ 9.47 (d, J_{HH} =

6, 2H), 9.163 (s, 2H), 9.06 (s, 2H), 8.28 (d, J_{HH} = 6, 2H), 7.94 (d, J_{HH} = 6, 2H), 7.69 (d, J_{HH} = 6, 2H), 4.67 (q, J_{HH} = 7, 2H), 4.57 (q, J_{HH} = 7, 2H), 1.37 (t, J_{HH} = 7, 3H).

3. Results and discussion

3.1. Synthesis

The dyes were synthesized from the corresponding dichloride precursors by initial abstraction of the chloride ligands through treatment with silver nitrate. This was found to give a better yield and cleaner product compared with simple reflux of the dichlorides with the sulfur-donor ligand, as it allowed a lower temperature and shorter reaction time. Satisfactory purity and yield for the ester and acid-substituted dyes was subsequently obtained through column chromatography.

3.2. Electrochemistry

The redox potentials of all processes for each complex are shown in Table 1. Dyes **1** - **3** all show one reversible oxidation, which increases in potential by around 0.2 V upon inclusion of the electron-withdrawing ester/acid groups on the bipyridines. The electrochemistry of complex **2** was studied in both 0.1 M TBABF$_4$/DMF and 0.3 M TBABF$_4$/DCM, with the oxidation of the complex found to be only partially reversible in DMF but fully reversible in DCM. This is likely to arise from DMF coordinating to the oxidized species and further evidence for this was observed during the spectroelectrochemical studies. The first two reductions for **1** - **3** are assigned to the bipyridyl ligands and these are again observed to shift to more positive potential for the acid and ester-substituted complexes. The third reduction in the study of **2** may be assigned to the dithiolene ligand, as this was similar to reduction observed in the electrochemistry of the uncomplexed ligand. Dyes **4** - **6** show one oxidation and three reductions, assigned as ruthenium-based and bipyridyl ligand-based respectively. The oxidation for **4** – **6** was more positive than for the analogous dyes **1**

– **3**, presumably due to the additional positive charge on the former. The ester derivative in this series (**5**) was also studied in DMF and DCM and the oxidation process was found to be only quasi-reversible in both solvents. This was further investigated using spectroelectrochemistry (*vide infra*). The oxidation and reduction potentials of **3** and **6** are sufficient for both regeneration by the iodide/triiodide redox electrolyte and injection into the conduction band of TiO_2, when compared with the expected energies of these components and hence both dyes expected to function as sensitizers in a DSSC.

3.3. Absorption spectroscopy

Absorption spectrawere recorded in DMF (Table 2; Figs. 2 and 3) and the assignment of these transitions have been further investigated using theoretical computational studies (Section 3.5). 1, 2 and 3 show a significant red-shift of the absorption maximum, peaking at 548 nm(1) and around 580nm(2,3) respectively, relative to complexes 4, 5, and 6 with corresponding peaks around 490 and 530 nm. This may be due to the strong electron donating character of the C2N2S2 ligand having the desired effect on the metal t2g orbitals, thereby decreasing the HOMO–LUMO gap. In comparison to N719, dye 3 shows a significantly lower absorption energy and hence a greater absorption range has been achieved as desired. The molar extinction co-efficients of the acid dyes (3 and 6) are both slightly higher than that of N719 [22], which not only increases their light harvesting efficiency relative to N719 but may also lead to the ability to produce thinner cells, a distinct advantage in a DSSC due to the decreased losses associated with charge transport [23]. Fluorescence studies showed that 1–3 showed no room temperature emission in ethanol whereas 4–6 showed weak emission. The S2COEt emission spectra (Table 2) did not overlap with the excitation spectra suggesting typical triplet emission as would be expected

for these types of complexes. The lack of any observable emission from 1 to 3 may suggest that there is not the typical MLCT emissive state present in these dyes. These findings are further discussed with respect to the density functional theory (DFT) calculations.

3.4. Spectroelectrochemistry

Through studying the oxidized and reduced species of these complexes the nature of the frontier orbitals can be further investigated. The change in absorption spectrum of **2** upon oxidation was studied in both 0.1 M $TBABF_4$/DMF and 0.3 M $TBABF_4$/DCM, firstly to establish whether the solvent was coordinating to the oxidized complex, as had been hypothesized from the electrochemical studies in the two solvents, and secondly to further characterize the nature of the HOMO. In DMF the CT bands were seen to decrease in intensity and gradually two new bands grew in, however no isosbestic points were observed between the initial and final spectra (Figure S1). This behavior was not fully reversible to the initial spectrum upon re-reduction, further evidence that the oxidized product is itself forming another species. In DCM the CT bands also decrease in intensity however there is no new peak growth (Figure 4). In addition to this, four isosbestic points are observed and the study was fully reversible back to the initial spectrum upon re-reduction. These studies, as well as the electrochemical studies, carried out in the two solvents strongly suggest that solvent coordination is playing a role upon oxidation of **2**. Therefore results in the non-coordinating solvent DCM will be used to discuss the oxidation of **2** in more detail rather than those obtained in the DMF study. As well as the partial collapse of the CT bands, the study in DCM also shows a broadening of the bipyridyl intraligand band, indicative of a ruthenium based oxidation.[7] The fact that the CT bands do not fully collapse, and also retain their peak shape suggests that the oxidation is not fully ruthenium based but perhaps has some degree of $C_2N_2S_2$ ligand character. The mono-

reduced and di-reduced species of **2** were studied in DMF (Table 3, Figure S1) and are very similar to that of the mono-reduced and di-reduced species of [Ru(decbpy)$_2$(CN)$_2$], suggesting that the lowest unoccupied orbitals are bipyridyl ligand in nature.[xi] The mono-reduced species shows collapse of the MLCT bands followed by the growth of new intraligand bands in their place. The π-π^* intraligand band at 31000 cm^{-1} completely collapses after di-reduction, and several of the features observed in the mono-reduced spectrum become more intense (Table 3) as was observed for Ru(decbpy)$_2$(CN)$_2$. The unsubstituted bipyridyl dye (**1**) in this series showed a similar result upon oxidation (Table 3, Figure S2) with the partial collapse of the CT bands and a broadening of the bipyridyl intraligand band and again the CT bands retained their peak shape, providing further evidence that the HOMO of the dyes in this series may have a significant degree of C$_2$N$_2$S$_2$ character.

The oxidative OTTLE experiment for **5** was also found to be solvent dependent, showing in DMF no well-defined isosbestic points and deviations from the original spectrum upon re-reduction. The study in DCM again showed a number of isosbestic points and fully reversible behavior. The oxidation of **5** in DCM (Figure 5, Table 3) showed an almost complete collapse of the lowest energy CT band and a partial collapse of the second CT band as well as a broadening of the bipyridyl intraligand band. Similar observations were made upon oxidation of [Ru(decbpy)$_2$Cl$_2$], indicating that the HOMO of **5** may be largely located on the ruthenium centre. The mono-reduced and di-reduced OTTLE studies of **5** closely resemble that of **2**, indicating that the reductions are bipyridyl ligand based (Figure S3). The unsubstituted bipyridyl analogue **4** again showed a similar solvent dependence and also indicated a largely ruthenium centered HOMO, with the complete collapse of the low energy CT band and a partial collapse of the second CT band (Table 3, Figure

S4). Also observed in this study was the complete collapse of the bipyridyl intraligand band along with the growth of another band at 31700 cm^{-1}. Upon comparison to the oxidation of [Ru(bpy)$_2$Cl$_2$] there are distinct similarities indicating a large contribution of the ruthenium to the HOMO.

Interestingly, spectroelectrochemical studies carried out on the ethyl ester analogue of N719 found that this dye is not stable in the oxidized state.[xii] In both DMF and DCM the oxidative study was found to be irreversible and hence the introduction of the bidentate S-donor ligands has indeed increased the stability of the dyes in the oxidized state as desired.

3.5. Hybrid DFT calculations

Density functional theory (DFT) and time-dependent DFT (TD-DFT) are computational techniques that have been used in a number studies to great effect to investigate the photophysical properties of ruthenium polypyridyl complexes.[xiii] Here, these techniques have been used to study the energies and composition of the frontier orbitals, as well as investigate the electronic transitions between these states for compounds **2** and **5**. Percentage contributions and energies of the frontier orbitals of **2** and **5** can be found in Table S1 and S2 in supporting information. The HOMO of **2** was found to be largely ruthenium in character (54 %) with partial delocalization over the C$_2$N$_2$S$_2$ ligand (39 %). In addition the HOMO-1 was found to be very close in energy, with only a 0.07 eV difference, and also shows significant delocalization over the C$_2$N$_2$S$_2$ ligand (Figure 6). This suggests that upon oxidation of the dye the resulting hole will be partly delocalized onto the entire ligand which may be advantageous in a DSSC for regeneration of the oxidized dye by the redox mediator and for reduced charge recombination. The large contribution of the C$_2$N$_2$S$_2$ ligand to the HOMO may also explain the lack of fluorescence observed with this dye series, as this would mean that the emissive state was not a typical MLCT and instead possesses

significant ligand-to-ligand charge-transfer character at lower energy. The lower-energy state would be expected to undergo more rapid non-radiative decay and therefore emission in fluid solution at room temperature is not observed. The lowest unoccupied orbitals were found to be located mainly over the two bipyridyl rings with a small degree of ruthenium character, which agrees very well with the reductive spectroelectrochemical studies.

Complex **5** was also calculated to have significant ruthenium contribution to the HOMO (62 %) however there was less delocalization over the dithiolene ligand in comparison to **2** (Figure 7). The HOMO-1 and HOMO-2 energy levels were found to be very close in energy with only a 0.06 eV difference between them. Both of these orbitals have a large degree of ruthenium character and only partial contributions from the bipyridyl and xanthate ligands. Again the LUMO was calculated to be located over the two bipyridyl ligands with a small degree of ruthenium character, which should facilitate efficient injection into the conduction band of the TiO_2.

TD-DFT calculations were also carried out for **2** and **5** with the calculated absorption spectra showing significant similarities to the observed. It should be noted that in this study the inclusion of solvent in these calculations was extremely important as vacuum calculations greatly underestimated the energy of the transitions, particularly the lowest energy MLCT bands, in line with previous TD-DFT studies on similar complexes.[xiv,xv] The energies, oscillator strengths and composition of the calculated transitions can be found in supporting information Table S3. The calculated transitions from a TD-DFT calculation can be converted to a simulated spectrum via a Gaussian convolution and this technique has previously been used successfully for ruthenium polypyridyl complexes.[xvi,xvii,xviii,xix] For **2** and **5** in DMF (Figure 8), the calculated and observed spectra have significant similarities. Firstly,

the bipyridyl transitions at ~ 300 nm were well reproduced both in energy of transition and intensity relative to other transitions. Interestingly, for both dyes the lowest energy band was found not to be HOMO-LUMO in nature but rather HOMO-2 to LUMO, making this band well described as MLCT in both cases, rather than a mixed ruthenium/S-donor ligand to bipyridyl ligand as would be the case for the HOMO-LUMO transitions. For both systems the character of the HOMO-2 is largely ruthenium, which leads to a greater degree of overlap with the unoccupied orbitals compared to the HOMO and HOMO-1. Importantly in comparing the two simulated spectra the observed trend of **2** having an extended absorption range was conserved with a calculated absorption maximum at 500 nm versus 470 nm for **5**. These results also relate well to the spectroelectrochemical studies of **2** and **5** carried out in 0.3 M TBABF$_4$/DCM. Upon oxidation of **2** it was observed that the CT bands decrease in intensity but do not fully collapse or shift in energy. This infers that removal of an electron from the HOMO does not affect the energies of the transitions significantly. In contrast the spectroelectrochemistry of **5** showed an almost complete collapse of the lowest energy CT band upon oxidation, reflecting the fact the highest occupied orbitals are all largely ruthenium in character and hence the oxidation of the ruthenium centre greatly alters these transitions.

3.6. Solar cell measurements

DSSCs incorporating dyes **3** and **6** were constructed and the performance of the cells investigated by measuring the IPCE (Figure 9, Table 4) and I-V curves, with the results compared to a cell with N719 as the sensitizer for reference. The IPCE curves for the two synthesized dyes show a clear resemblance to the absorption spectra, showing no significant decomposition upon adsorption or in contact with the electrolyte and that the characterization in solution relates well to that of the dye/TiO$_2$

system. The maximum IPCE of **3** at 555 nm was unexpectedly low at 11 %, whereas in comparison **6** yielded a value almost three times greater of 29 % at 520 nm. The possibility that this was due to dye aggregation upon sensitization was investigated by using a much more dilute dye bath, however this cell gave a comparable low efficiency showing that this is unlikely to be the major cause.

The overall efficiency (η) of a solar cell can be quantified using equation 1, with the values of short circuit current (I_{sc}), open circuit voltage (V_{oc}) and fill factor (ff) taken from an I-V curve and the power input (P_{in}) being the intensity of the incident light (1000 W/m^2).

$$\eta_{cell} = \frac{I_{sc}V_{oc}\,ff}{P_{in}}$$

The I-V curves for the three different dyes are shown in Figure 10 and the resulting values of I_{sc}, V_{oc}, ff and η obtained, in Table 4. As expected from the IPCE results the cell made with **3** was found to be very low efficiency at 0.4 % and the cell made with **6** three times greater at 1.2 %. For comparison the cell with N719 as the sensitizer gave an efficiency of 2.1 %. These results show that whilst both dyes do function in a DSSC, there is clearly some limiting factor in the case of **3** resulting in a low efficiency cell.

Following the encouraging efficiency of **6**, we attempted to optimize the cell to enhance the efficiency. This was rather disappointing however, with the efficiency using **6** rising to 1.88 % using conditions that gave 6.4 % for N719. It is not clear at present whether this represents a true limit to the efficiency of **6** or whether different optimization conditions would be needed to reflect its different electronic character (for example the different charge). Details of the cell optimization conditions and results can be found in supplementary information.

3.7. Transient absorption spectroscopy

In order to rationalize the differing efficiencies of 3 and 6 in a DSSC the kinetics of the TiO2/dye system were investigated using transient absorption spectroscopy. The excitation wavelength was set at 500 nm, a wavelength at which the two sensitized films absorbed approximately the same number of photons. A probe wavelength of 600 nm was chosen, where the ground state bleach recovery of the dyes can be easily monitored and the lifetime of the dye cations inferred. The recombination of the injected electrons with the oxidized dye was investigated using a redox inactive electrolyte (0.25M LiClO4 in propylene carbonate). Complex 3 showed very fast recombination kinetics with a half lifetime on the order of 10μs, which was about 1000 times faster than the recombination dynamics observed for complex 6, with t1/2 in the order of a fewmilliseconds. Fromthe DFT and spectroelectrochemical studies

it would have been expected that the recombination loss process would have been much slower in 3 compared to 6, as the dye cation hole is thought to be considerably delocalized over the C2N2S2 ligand. This would mean that if the dyewere binding through the acid groups with the C2N2S2 ligand pointing away fromthe TiO2 surface, the injected electrons would take longer to recombine with the oxidized dye because the hole is located further from the surface, as has been observed previously [32]. The fact that the opposite has been observed suggests that the dye is binding in amode that facilitates much faster recombination, a simple answer to that being through the terminal cyano group on the C2N2S2 ligand. If there is concerted binding through both the acid and cyano groups then this would account for the low IPCE and low _ through fast recombination as the injected electrons will readily recombine with the oxidized dye if the dye cation hole is close to the surface of the TiO2. The regeneration of the oxidized dyes was investigated by covering the sensitized films with a redox active electrolyte, 0.25M LiI/0.05M I2 in propylene carbonate (Figs. S6

and S7). As would be expected for a dye that has shown significant efficiencies in a DSSC, dye 6 showed very efficient regeneration dynamics, with a half lifetime for the oxidized dye of only a few microseconds, in the same timescale as the regeneration dynamics of the standard N719 [33], and about 1000 times faster than the recombination kinetics. On the other hand, complex 3 showed regeneration dynamics

one order of magnitude slower, with t1/2 of tens of microseconds, which is on the same timescale as the observed recombination kinetics for this dye and indicates that recombination with the injected electrons is competing with regeneration of the oxidized dyes by the electrolyte in the DSSC, lowering the efficiency of the device. The faster regeneration dynamics of complex 6 compared to 3 can be attributed to its more positive oxidation potential and therefore, to the larger driving force for the regeneration process (Fig. 11).

3.8. TiO2/dye absorption study

To investigate the possibility of the cyano group on the C2N2S2 ligand binding to the TiO2 in addition to the acid groups, the unsubstituted and ester derivative dyes were used to sensitize TiO2 films and in addition the bis-chloride complexes and ethyl xanthate dyes were used as further evidence. The films were soaked overnight

in a 1mM solution in methanol, and rinsed with methanol before absorption spectra were recorded. For the unsubstituted and ester bipyridyl dyes containing the chloride ligands the dye uptake was very low with a maximum absorbance below 0.1 and in the case of the ethyl xanthate series therewas no measurable absorbance. This shows these dyes have very little or negligible binding to the TiO2 without the presence of the acid groups on the bipyridyl ligands. With the C2N2S2 series the dye loading was much greater (Fig. 12), with the absorption values of the unsubstituted and ester dyes virtually identical at ~0.15, compared to an absorbance of ~0.9 for the acid derivative. Overall, this study strongly suggests that the cyano group is capable of reasonably

strong interaction with the TiO2 surface. This suggests that for the sensitizer 3, the cyano group may be interacting with the TiO2 in addition to the usual binding through

the acid groups, resulting in very fast recombination in a DSSC and

a low efficiency cell.

4. Summary

Two novel series of ruthenium bipyridyl dyes containing S donor ligands have been synthesized and characterized. The properties of the two series are very distinct with the C2N2S2 series showing significant HOMO contribution from the sulfur-donor ligand and the S2COEt series having a HOMO largely located on the ruthenium centre. This reflects the greater conjugation across the former ligand. The dianionic C2N2S2 ligand also displays greater electron donating capability than the monoanionic S2COEt, resulting in destabilization of themetal d-orbitals and lower energyMLCT transitions that also possess a high molar extinction coefficient. Thus Ru(dcbpy)2(C2N2S2) has a number of advantageous properties for a DSSC sensitizer including an expected higher light harvesting capability in the visible range and delocalization of the HOMO to enhance charge separation. Despite these characteristics, it performed worse with respect to [Ru(dcbpy)2(S2COEt)]+ in a DSSC. This is attributed to the terminal cyano group of the C2N2S2 ligand binding to the surface of the TiO2 in addition to the acid groups on the bipyridyl ligands, facilitating fast recombination of the injected electron with the oxidized dye. In contrast, [Ru(dcbpy)2(S2COEt)]+ showed an efficiency of 1.2% in an unoptimized DSSC. It is apparent that complexes within this family can possess very attractive features for sensitizers in DSSC. Modification of the sulfur-donor ligand has been shown to enable enhanced electronic characteristics and chelating ligands can offer

enhanced dye stability. An additional point to note is the possible variation of the alkyl chain length on the S2COEt ligand, since hydrophobicity in dyes has been associated with enhanced stability [34], reduction of charge recombination with the electrolyte [35,36] and good interaction with the organic hole-transportmaterials used in solid-state cells [2]. The challenge for subsequent studies will be the combination of these various positive features into a dye,while avoiding inadvertent detrimental effects such as the rapid recombination observed for 3.

Acknowledgements

References

[1] B. O'Regan, M. Gratzel, Nature 353 (1991) 737–739.

[2] N. Roberston, Angew. Chem. Int. Ed. 45 (2006) 2338–2345.

[3] Md.K. Nazeeruddin, F. De Angelis, S. Fantacci, A. Selloni, G. Viscardi, P. Liska, S.

Ito, B. Takeru, M. Gratzel, J. Am. Chem. Soc. 127 (2005) 16835–16847.

[4] Md.K. Nazeeruddin, M. Gratzel, Comp. Coord. Chem. II 9 (2003) 719–758.

[5] P.A. Anderson, G.F. Strouse, J.A. Treadway, F.R. Keene, T.J. Meyer, Inorg. Chem.

33 (1994) 3863–3864.

[6] K. Kalyanasundaram,Md.K.Nazeeruddin, Chem. Phys. Lett. 193 (1992) 292–297.

[7] R. Argazzi, C.A. Bignozzi, T.A. Heimer, F.N. Castellano, G.J. Meyer, Inorg. Chem.

33 (1994) 5741–5749.

[8] A. Islam, K. Hara, L.P. Singh, R. Katoh, M. Yanagida, S. Murata, Y. Takahashi, H.

Sugihara, H. Arakawa, Chem. Lett. (2000) 490–491.

[9] H. Greijer Agrell, J. Lindgren, A. Hagfeldt, Solar Energy 75 (2003) 169–180.

[10] R. Argazzi, C.A. Bignozzi, G.M. Hasselmann, G.J. Meyer, Inorg. Chem. 37 (1998)

4533–4537.

[11] A. Islam, H. Sugihara, K. Hara, L.P. Singh, R. Katoh, M. Yanagida, Y. Takahashi, S.

Murata, H. Arakawa, J. Photochem. Photobiol. A: Chem. 145 (2001) 135–141.

[12] B.P. Sullivan, D.J. Salmon, T.J. Meyer, Inorg. Chem. 17 (1978) 3334–3341.

[13] G.Wolfbauer, A.M. Bond, D.R. MacFarlane, Inorg. Chem. 38 (1999) 3836–3846.

[14] C.J. Burchell, S.M. Aucott, H.L. Milton, A.M.Z. Slawin, J.D.Woollins, Dalton Trans.

(2004) 369–374.

[15] M.J. Frisch, G.W. Trucks, H.B. Schlegel, G.E. Scuseria, M.A. Robb, J.R. Cheeseman,

J.A. Montgomery Jr., T. Vreven, K.N. Kudin, J.C. Burant, J.M. Millam, S.S.

Iyengar, J. Tomasi, V. Barone, B. Mennucci, M. Cossi, G. Scalmani, N. Rega, G.A.

Petersson, H. Nakatsuji, M. Hada, M. Ehara, K. Toyota, R. Fukuda, J. Hasegawa,

M. Ishida, T. Nakajima, Y. Honda, O. Kitao, H. Nakai, M. Klene, X. Li, J.E. Knox, H.P.

Hratchian, J.B. Cross, V. Bakken, C. Adamo, J. Jaramillo, R. Gomperts, R.E. Stratmann,

O. Yazyev, A.J. Austin, R. Cammi, C. Pomelli, J.W. Ochterski, P.Y. Ayala, K.

Morokuma, G.A. Voth, P. Salvador, J.J. Dannenberg, V.G. Zakrzewski, S. Dapprich,

A.D. Daniels, M.C. Strain, O. Farkas, D.K. Malick, A.D. Rabuck, K. Raghavachari,

J.B. Foresman, J.V. Ortiz, Q. Cui, A.G. Baboul, S. Clifford, J. Cioslowski, B.B. Stefanov,

G. Liu, A. Liashenko, P. Piskorz, I. Komaromi, R.L. Martin, D.J. Fox, T. Keith,

M.A. Al-Laham, C.Y. Peng, A. Nanayakkara, M. Challacombe, P.M.W. Gill, B. Johnson,

W. Chen, M.W. Wong, C. Gonzalez, J.A. Pople, Gaussian 03, Revision C.02, Gaussian, Inc.,Wallingford, CT, 2004.

[16] J.P. Perdew, J.A. Chevary, S.H. Vosko, K.A. Jackson, M.R. Pederson, D.J. Singh, C. Fiolhais, Phys. Rev. B 48 (1993) 4978–14978.

[17] J.P. Perdew, K. Burke, Y.Wang, Phys. Rev. B 54 (1996) 16533–16539.

[18] P.J. Hay,W.R.Wadt, J. Chem. Phys. 82 (1985) 299–310.

[19] M.M. Francl, W.J. Pietro, W.J. Hehre, J.S. Binkley, M.S. Gordon, D.J. Defrees, J.A. Pople, J. Chem. Phys. 77 (1982) 3654–3665.

[20] E.S. Boes, P.R. Livotto, H. Stassen, Chem. Phys. 331 (2006) 142–158.

[21] N. Papageorgiou, W.F. Maier, M. Gratzel, J. Electrochem. Soc. 144 (1997) 876–884.

[22] Md.K. Nazeeruddin, A. Kay, I. Rodicio, R. Humphry-Baker, E. Muller, P. Liska, N. Vlachopoulos, M. Gratzel, J. Am. Chem. Soc. 115 (1993) 6382–6390.

[23] L. Schmidt-Mende, U. Bach, R. Humphry-Baker, T. Horiuchi, H. Miura, S. Ito, S. Uchida, M. Gratzel, Adv. Mater. 17 (2005) 813–815.

[24] G.Wolfbauer, A.M. Bond, D.R. MacFarlane, Dalton Trans. (1999) 4363–4372.

[25] K.L. McCall, N. Robertson, unpublished work.

[26] A. Vlˇcek Jr., S. Zalis, Coord. Chem. Rev. 251 (2007) 258–287.

[27] A. Vlˇcek Jr., S. Zalis, J. Phys. Chem. A 109 (2005) 2991–2992.

[28] M.-F. Charlot, A. Aukauloo, J. Phys. Chem. A 111 (2007) 11661–11672.

[29] F. De Angelis, S. Fantacci, A. Selloni, Md.K. Nazeeruddin, Chem. Phys. Lett. 415

(2005) 115–120.

[30] S.R. Stoyanov, J.M. Villegas, D.P. Rillema, Inorg. Chem. Commun. 7 (2004)

838–841.

[31] Y. Xu, W.-K. Chen, M.-J. Cao, S.-H. Liu, J.-Q. Li, A.I. Philippopoulos, P. Falaras,

Chem. Phys. 330 (2006) 204–211.

[32] S. Handa, H. Wietasch, M. Thelakkat, J.R. Durrant, S.A. Haque, Chem. Commun.

(2007) 1725–1727.

[33] J.N. Clifford, E. Palomares, Md.K. Nazeeruddin, M. Gratzel, J.R. Durrant, J. Phys.

Chem. C 111 (2007) 6561–6567.

[34] Md.K. Nazeeruddin, S.M. Zakeeruddin, J.-J. Lagref, P. Liska, P. Comte, C. Barolo,

G. Viscardi, K. Schenk, M. Gratzel, Coord. Chem. Rev. 248 (2004) 1317–1328.

[35] S.M. Zakeeruddin, Md.K. Nazeeruddin, R. Humphry-Baker, P. Pechy, P.

Quagliotto, C. Barolo, G. Viscardi, M. Gratzel, Langmuir 18 (2002) 952–954.

[36] L. Schmidt-Mende, J.E. Kroeze, J.R. Durrant, Md.K. Nazeeruddin, M. Gratzel,

Nano Lett. 5 (2005) 1315–1320.

Table 1. Redox potentials of oxidative and reduction processes in 0.1 M
TBABF$_4$/DMF (vs. Ag/AgCl) for all complexes.

Complex	$E_{1/2}^{ox}$ / V	$E_{1/2}^{red}$ / V		
Ru(bpy)$_2$(C$_2$N$_2$S$_2$) (**1**)	0.52	-1.44	-1.75	-
Ru(decbpy)$_2$(C$_2$N$_2$S$_2$) (**2**)	0.73	-0.98	-1.21	-1.77 [a]

Complex				
Ru(dcbpy)$_2$(C$_2$N$_2$S$_2$) (3)	0.71	-1.08 [a]	-1.34 [a]	-
[Ru(bpy)$_2$(S$_2$COEt)][NO$_3$] (4)	0.89	-1.33	-1.6	-
[Ru(decbpy)$_2$(S$_2$COEt)][NO$_3$] (5)	1.07 [b]	-0.90	-1.09	-1.68 [a]
[Ru(dcbpy)$_2$(S$_2$COEt)][NO$_3$] (6)	1.08 [b]	-0.83 [a]	-1.08 [a]	-1.58 [a]

[a] Irreversible

[b] Quasi-reversible

Table 2. Summary of absorption spectra and emission maxima of all complexes carried out in DMF and ethanol respectively. Molar extinction co-efficients / 10^3 mol^{-1} cm^{-1} shown in brackets.

Complex	$\pi-\pi^*$/nm	MLCT/nm			Emission max. / nm
Ru(bpy)$_2$(C$_2$N$_2$S$_2$) (1)	298 (51.3)	548 (8.9)	481 sh (6.4)	361 (14.6)	-
Ru(decbpy)$_2$(C$_2$N$_2$S$_2$) (2)	320 (45.2)	583 (15)	417 (14.2)	361 (13.7)	-
Ru(dcbpy)$_2$(C$_2$N$_2$S$_2$) (3)	319 (39)	578 (13)	408 (14.3)	364 (13.2)	-
Ru(bpy)$_2$(S$_2$COEt) (4)	292 (56)	492 (8.9)	447 sh (7)	357 (8.8)	690
Ru(decbpy)$_2$(S$_2$COEt) (5)	317 (48.9)	530 (15.5)	463 sh (11.6)	396 (14.5)	760
Ru(dcbpy)$_2$(S$_2$COEt) (6)	314 (48.6)	528 (15.2)	463 (10.1)	391 (15.0)	750

Table 3. Absorption spectra maxima of electrochemically mono-oxidized, mono-reduced and di-reduced **2** and **5**.

Complex	Absorption / cm^{-1} (ε / mol^{-1} cm^{-1} 10^3)
[Ru(decbpy)$_2$(C$_2$N$_2$S$_2$)]$^+$	17400 (5.6) 19900 (6.7) 22150 (7.6) 24700 (9.3) 31850 (37.9) 40250 (33.2)
[Ru(decbpy)$_2$(C$_2$N$_2$S$_2$)]$^-$	6012 (5.8) 15205 (7.4) 18323 (11.6) 19842 (15.7) 20960 (16.2) 27755 (24.3) 31193 (25.0)

$[Ru(decbpy)_2(C_2N_2S_2)]^{2-}$ 6293 (14.2) 20890 (20.2) 25263 (19.4) 28093 (31.1)

$[Ru(bpy)_2(C_2N_2S_2)]^{+}$ 15153 (1.3) 21627 (4.1) 28839 (9.1) 31577 (17.8) 33758 (36.4)

$[Ru(decbpy)_2(S_2COEt)]^{2+}$ 19818 (3.67) 25825 (8.3) 30092 (21.8) 31655 (34.2)

$[Ru(bpy)_2(S_2COEt)]^{2+}$ 14750 (1.6) 29100 (6.0) 31700 (26.1) 33000 (23.6) 40500 (29.1)

$[Ru(decbpy)_2(S_2COEt)]$ 6233 (2.9) 16897 (9.7) 18454 (11.1) 22808 (14.4) 26666 (14.6) 31209 (32.7)

$[Ru(decbpy)_2(S_2COEt)]^{-}$ 6384 (9.7) 20875 (19.5) 28215 (29.3)

Table 4. IPCE maxima and short-circuit current, open-circuit voltage, fill factor and overall efficiency of DSSCs sensitized with **3**, **6** and N719 dyes.

Dye	IPCE max. / % (λ / nm)	I_{sc} / mA	V_{oc} / mV	ff	η / %
3	11.3 (555)	1.79	464	0.49	0.41
6	28.5 (517)	3.72	569	0.56	1.19
N719	39.9 (520)	5.37	637	0.62	2.12
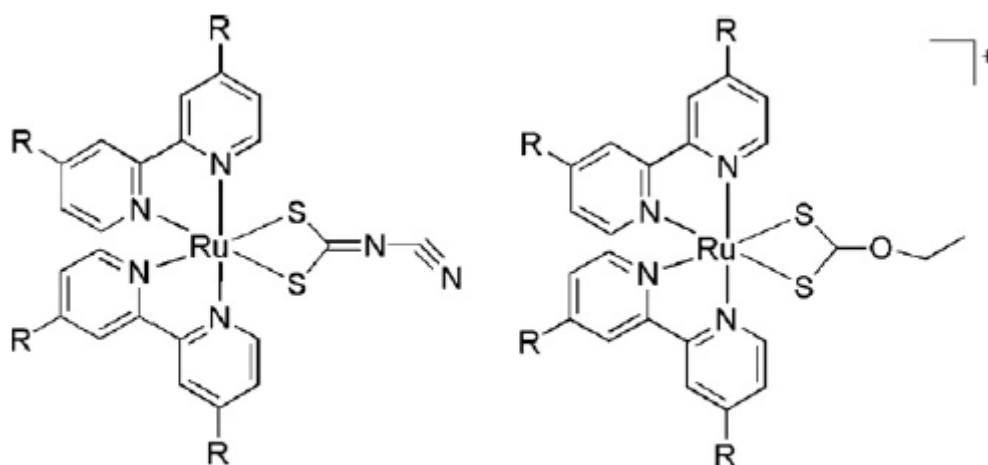
R = -H, -CO$_2$Et, -CO$_2$H

Figure 1. Chemical structures of [Ru(R-bpy)$_2$C$_2$N$_2$S$_2$] (R = H (**1**), CO$_2$Et (**2**), CO$_2$H (**3**)) and [Ru(R-bpy)$_2$(S$_2$COEt)][NO$_3$] (R = H (**4**), CO$_2$Et (**5**), CO$_2$H (**6**))
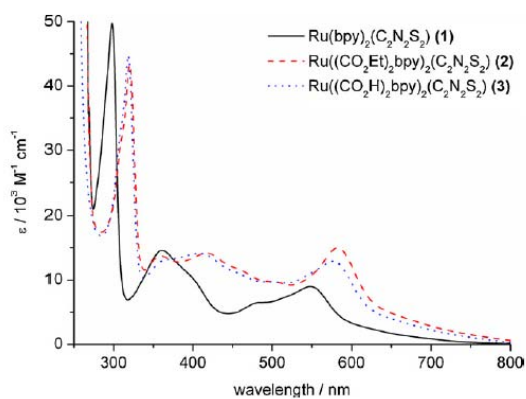
Figure 2.
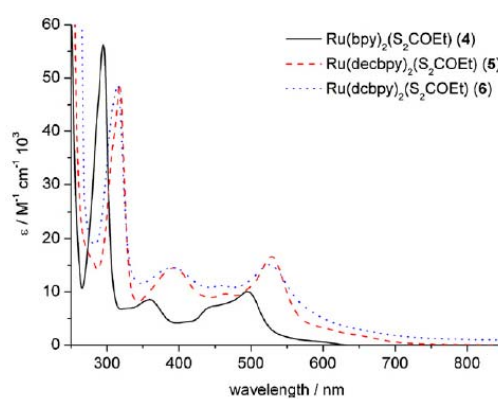
Figure 3

Figure 2. Absorption spectra of complexes **1** – **3**, in DMF.

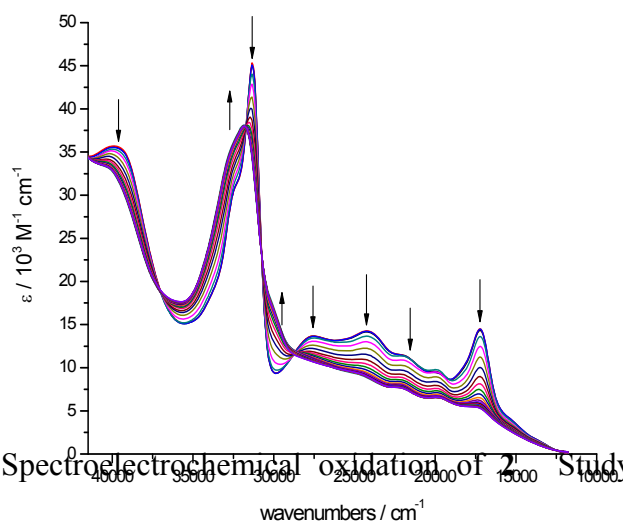**Figure 3.** Absorption spectra of complexes **4** – **6**, in DMF.

Figure 4. Spectroelectrochemical oxidation of **2**. Study carried out in 0.3 M TBABF$_4$/DCM at -40 °C, with an applied potential of + 1 V (vs. Ag/AgCl). Arrows indicate the growth or reduction of an absorption band with oxidation.
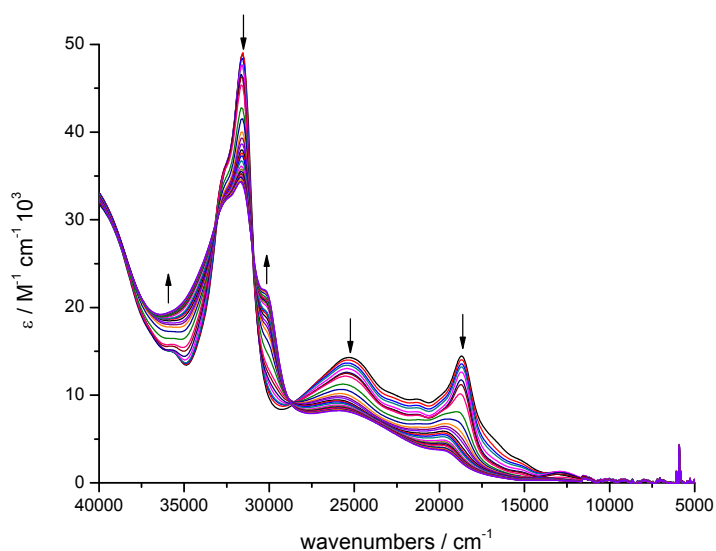
Figure 5. Spectroelectrochemical oxidation of **5**. Study carried out in 0.3 M TBABF$_4$/DCM at -40 °C, with an applied potential of + 1.5 V (vs. Ag/AgCl). Arrows indicate the growth or reduction of an absorption band with oxidation.
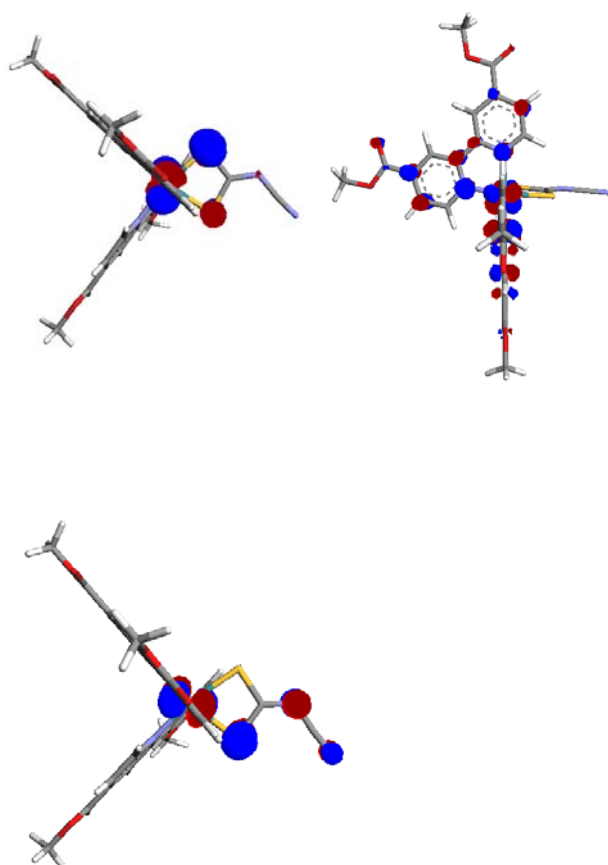
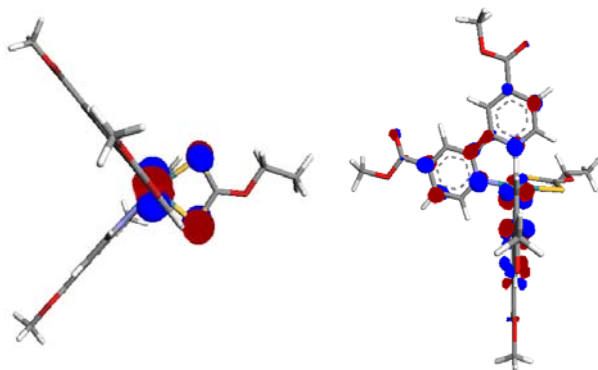**Figure 6.** Calculated a) HOMO, b) LUMO and c) HOMO-1 of **2** in DMF.

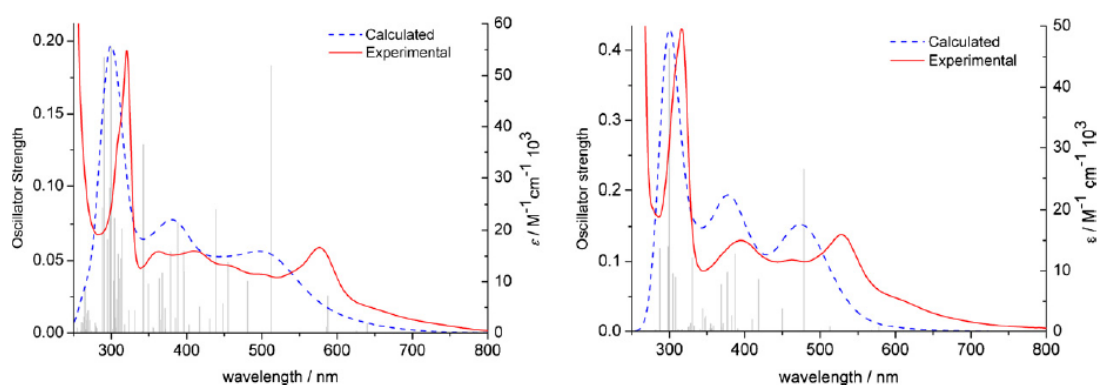**Figure 7.** Calculated a) HOMO and b) LUMO of **5** in DMF

Figure 8. Calculated electronic transitions (columns) for (left) **2** and (right) **5** relative to observed spectra (red solid line graph) and calculated spectra (blue dashed line graph).
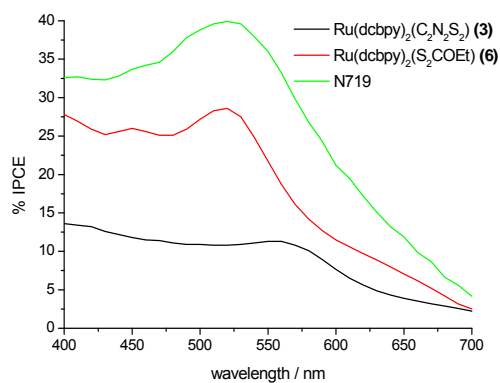

Figure 9. IPCE graphs for **3**, **6** and **N719** DSSCs, using 0.6 M PMII, 0.03 M I$_2$, 0.1 M guanidinium thiocyanate, 0.5M TBP in acetonitrile/valeonitrile as the redox electrolyte.
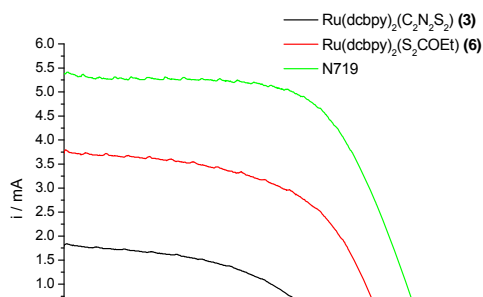
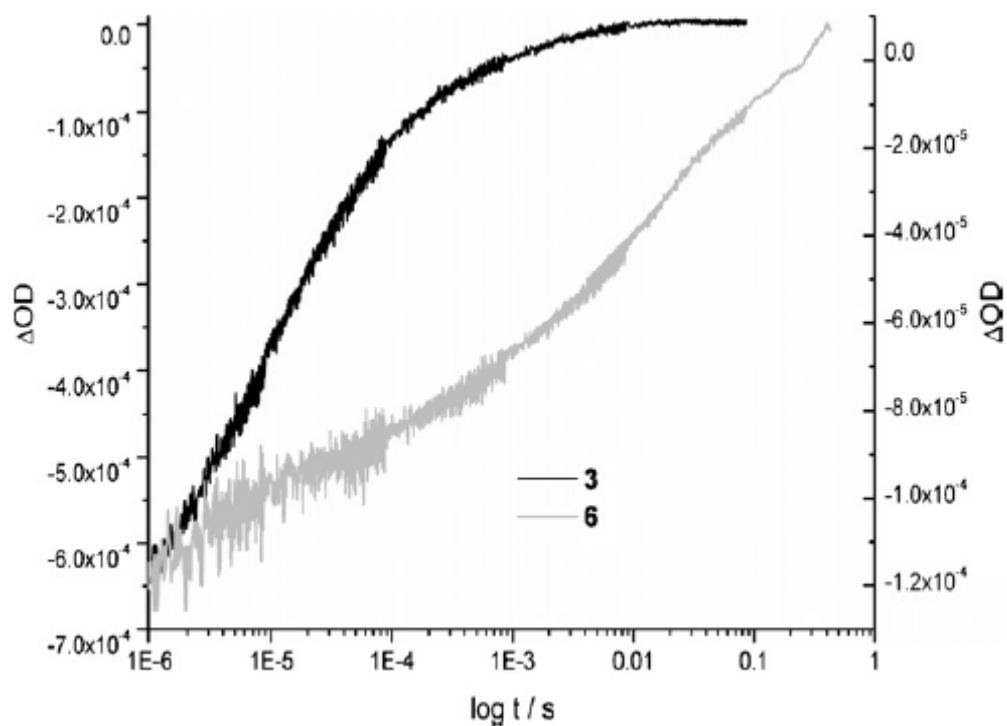**Figure 10**. Plot of I vs. V for **3**, **6** and N719 DSSCs

Fig. 11. Ground state bleach recovery of dye 3 sensitized TiO2 (black, left axis) and
dye 6 sensitized TiO2 (gray, right axis) monitored by transient absorption. The
recovery is due to the recombination of the oxidized dyes with the TiO2 electrons. The
excitation and probe wavelengths are 500 and 600 nm, respectively. The samples
are covered by a redox inactive electrolyte (0.25M LiClO4 in propylene carbonate).
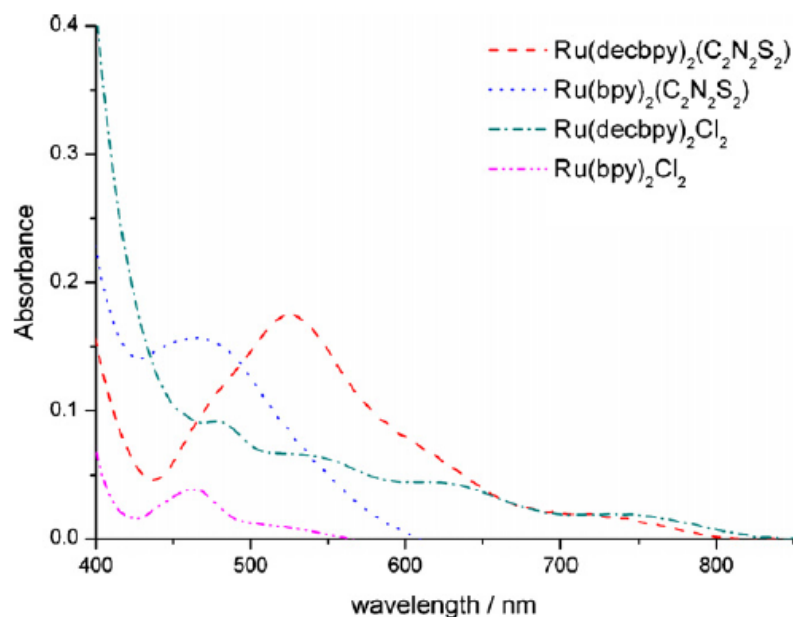
Fig. 12. Absorption spectra of dye/TiO2 films of C2N2S2 series and bis-chloride starting
materials.

[i] Sullivan, B.P.; Salmon, D.J.; Meyer, T.J.; *Inorg. Chem.,* **1978**, *17,* 3334-3341.

[ii] Wolfbauer, G.; Bond, A.M.; MacFarlane, D.R.; *Inorg. Chem.,* **1999**, *38*, 3836-3846.

[iii] Burchell, C.J.; Aucott, S.M.; Milton, H.L.; Slawin, A.M.Z.; Woollins, J.D.; *Dalton Trans.,* **2004**, 369-374.

[iv] Gaussian 03, Revision C.02, M. J. Frisch, G. W. Trucks, H. B. Schlegel, G. E. Scuseria, M. A. Robb, J. R. Cheeseman, J. A. Montgomery, Jr., T. Vreven, K. N. Kudin, J. C. Burant, J. M. Millam, S. S. Iyengar, J. Tomasi, V. Barone, B. Mennucci, M. Cossi, G. Scalmani, N. Rega, G. A. Petersson, H. Nakatsuji, M. Hada, M. Ehara, K. Toyota, R. Fukuda, J. Hasegawa, M. Ishida, T. Nakajima, Y. Honda, O. Kitao, H. Nakai, M. Klene, X. Li, J. E. Knox, H. P. Hratchian, J. B. Cross, V. Bakken, C. Adamo, J. Jaramillo, R. Gomperts, R. E. Stratmann, O. Yazyev, A. J. Austin, R. Cammi, C. Pomelli, J. W. Ochterski, P. Y. Ayala, K. Morokuma, G. A. Voth, P. Salvador, J. J. Dannenberg, V. G. Zakrzewski, S. Dapprich, A. D. Daniels, M. C.

Strain, O. Farkas, D. K. Malick, A. D. Rabuck, K. Raghavachari, J. B. Foresman, J. V. Ortiz, Q. Cui, A. G. Baboul, S. Clifford, J. Cioslowski, B. B. Stefanov, G. Liu, A. Liashenko, P. Piskorz, I. Komaromi, R. L. Martin, D. J. Fox, T. Keith, M. A. Al-Laham, C. Y. Peng, A. Nanayakkara, M. Challacombe, P. M. W. Gill, B. Johnson, W. Chen, M. W. Wong, C. Gonzalez, and J. A. Pople, Gaussian, Inc., Wallingford CT, 2004.

[v] Perdew, J.P.; Chevary, J.A.; Vosko, S.H.; Jackson, K.A.; Pederson, M.R.; Singh, D.J.; Fiolhais, C.; *Phys. Rev. B*, **1993**, *48*, 4978-4978.

[vi] Perdew, J.P.; Burke, K.; Wang, Y.; *Phys. Rev. B*, **1996**, *54*, 16533-16539.

[vii] Hay, P.J.; Wadt, W.R.; *J. Chem. Phys.*, **1985**, *82*, 299-310.

[viii] Francl, M.M.; Pietro, W.J.; Hehre, W.J.; Binkley, J.S.; Gordon, M.S.; Defrees, D.J.; Pople, J.A.; *J. Chem. Phys.,* **1982**, *77*, 3654-3665.

[ix] Boes, E.S.; Livotto, P.R.; Stassen, H.; *Chem. Phys.*, **2006**, *331*, 142-158.

[x] Papageorgiou, N.; Maier, W.F.; Grätzel, M.; *J. Electrochem. Soc.,* **1997,** *144*, 876-884.

[xi] Wolfbauer, G.; Bond, A.M.; MacFArlane, D.R.; *Dalton Trans.,* **1999**, 4363-4372.

[xii] McCall, K.L.; Robertson, N.; *Unpublished work.*

[xiii] Vlček Jr., A; Zális, S; *Coord. Chem. Rev.,* **2007**, *251*, 258-287.

[xiv] Vlček Jr., A; Zális, S; *J. Phys. Chem. A,* **2005**, *109,* 2991-2992.

[xv] Charlot, M-F.; Aukauloo, A.; *J. Phys. Chem. A*, **2007**, *111*, 11661-11672.

[xvi] Nazeeruddin, Md.K.; De Angelis, F.; Fantacci, S.; Selloni, A.; Viscardi, G.; Liska, P.; Ito, S.; Takeru, B.; Grätzel, M.; *J. Am. Chem. Soc.*, **2005**, *127*, 16835-16847.

[xvii] De Angelis, F.; Fantacci, S.; Selloni, A.; Nazeeruddin, Md.K.; *Chem. Phys. Lett.*, **2005**, *415*, 115-120.

[xviii] Stoyanov, S.R.; Villegas, J.M.; Rillema, D.P.; *Inorg. Chem. Commun.,* **2004**, *7*, 838-841.

[xix] Xu, Y.; Chen, W-K. ; Cao, M-J.; Liu, S-H.; Li, J-Q.; Philippopoulos, A.I. ; Falaras, P. ; *Chem. Phys.,* **2006**, *330*, 204-211.